Chiang Mai J. Sci. 2018; 45(5) : 2015-2020
http://epg.science.cmu.ac.th/ejournal/
Contributed Paper

Effects of Sintering Temperature on Physical Properties, Phase, Microstructure and Oxygen Stoichiometry of Na_yCoO_2 Ceramics

Pimpilai Wannasut [a,b], Paitoon Boonsong [a,b], Poom Prayoonphokkharat [a,b], Nittaya Keawprak [c] and Anucha Watcharapasorn* [a,d]

[a] Department of Physics and Materials Science, Faculty of Science, Chiang Mai University, Chiang Mai 50200, Thailand.

[b] Graduate PhD's Degree Program in Materials Science, Faculty of Science, Chiang Mai University, Chiang Mai 50200, Thailand.

[c] Thailand Institute of Scientific and Technological Research, Pathum Thani 12120, Thailand.

[d] Center of Excellence in Materials Science and Technology, Materials Science Research Center, Faculty of Science, Chiang Mai University, Chiang Mai 50200, Thailand.

* Author for correspondence; e-mail: anucha@stanfordalumni.org

Received: 1 November 2017
Accepted: 30 April 2018

ABSTRACT

Due to the stability in air, low cost and non-toxicity, oxide thermoelectrics have been considered a potential candidate for high-temperature waste-heat recovery devices. In this study, the effects of sintering temperature on phase, microstructure and oxygen content of Na_yCoO_2 (NCO) ceramics were investigated. The NCO ceramics were prepared by conventional solid-state reaction and sintering methods. The sintering condition included a temperature range of 800-950 °C and 18 h sintering time. The ceramic with a highest density value of 4.76 g/cm^3 was obtained by being sintered at 900 °C with the linear shrinkage of ~12%. X-ray diffractometry and Raman spectroscopy were used for phase analysis. The microstructure was determined by scanning electron microscopy. The change in oxygen stoichiometry was discussed in relation with the crystal structure and microstructural characteristics in order to elucidate the stability of this compound for high-temperature operation of thermoelectric device.

Keywords: oxide thermoelectrics, sodium cobalt oxide, conventional sintering

1. INTRODUCTION

Thermoelectric materials have become a promising candidate for many electronic devices such as refrigerator, electricity generator and boiler [1, 2]. Sodium cobalt oxide (Na_yCoO_2 or NCO) has been found to possess attractive thermoelectric properties such as high electrical conductivity, moderately high Seebeck coefficient and low thermal conductivity which resulted in high thermoelectric figure of merit (ZT) at high temperature [3, 4]. Nevertheless, the previously reported bulk NCO compound

indicated that a wide range of thermoelectric properties was possible. For examples, the electrical conductivity values could range from 5000-30000 $(ohm\text{-}m)^{-1}$, Seebeck coefficient could have a range of 50-300 μV/K or thermal conductivity could have the values of 0.5-5 W/mK, which resulted in a large variation in the reported ZT values at high temperature (i.e. 0.3-0.8 at 600 K) [5].

Due to the fact that, in most previously reported bulk NCO ceramics, the effects of phase compositions, microstructure and oxygen stoichiometry of NCO ceramics were rarely mentioned and used to elucidate why such a wide range of thermoelectric properties occurred, this work therefore attempted to investigate in details the effects of sintering condition on these factors in order to understand how they influenced the properties of Na_yCoO_2 ceramics.

2. MATERIALS AND METHODS

The starting materials for Na_yCoO_2 with y = 0.6 powder were Na_2CO_3 (99.5%, Riedel-de Ha-n) and Co_3O_4 (99.5%, Aldrich) powders. The powders were weighed and mixed by wet ball milling in ethanol (99% purity) for 24 h. The mixture was dried in an oven for 24 h, calcined at 750 °C for 16 h and then uniaxially pressed into cylindrical pellets. The green pellets were sintered at 800-950 °C for 18 h under normal air atmosphere. The densities were measured by a direct measurement of mass and volume.

An X-ray diffractrometer (XRD, Lab X-6000) was used for phase characterization. The quantitative analysis of phases present in the sample was carried out based on the experimental XRD patterns and Powder Cell 2.4 program [7]. The Raman spectra were obtained on polished sintered pellets using a Raman spectrometer (T6400 JY, Horiba Jobin Yvon, Horiba Ltd., Kyoto, Japan). A scanning electron microscope (SEM, JEOL JSM-6335F) was used for microstructural analysis.

3. RESULTS AND DISCUSSION

The values of density and linear shrinkage of NCO ceramics sintered at 800, 850, 900 and 950 °C for 18 h are shown in Figure 1. The highest density and linear shrinkage obtained for the sample sintered at 900 °C were 4.76 g/cm^3 (~96% relative density) and 11.07%, respectively. This seemed to be the optimum sintering condition in which the diffusion reaction between grains could be complete with moderate grain growth with respect to its reported melting point of 1000 °C [7, 8]. However, it may be noted that the true melting point may be higher or lower depending on the exact composition of NCO.

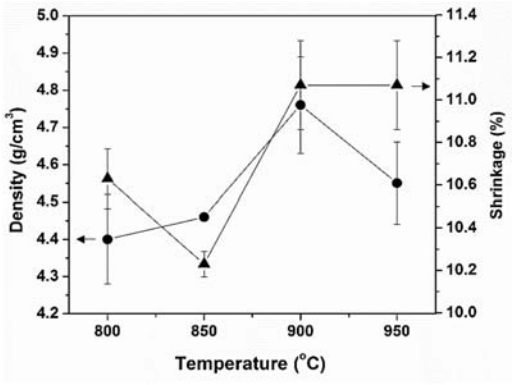

Figure 1. The densities and linear shrinkage of NCO ceramics at various sintering temperatures.

The experimental XRD patterns superimposed by the simulated XRD patterns obtained using the Powder Cell 2.4 program are shown in Figure 2. The simulated intensity values fitted to the actual XRD data with the Rietveld discrepancy values for R_p (R-pattern), R_{wp} (R-weighted pattern) and χ^2 (goodness-of-fit) are also indicated in the figure. The quality of

Rietveld refinement was quite satisfactory [9]. All of the $Na_{0.6}CoO_2$ ceramic samples could be indexed with a hexagonal unit cell in the space group $P6_3/mmc$ (No. 194) similar to that in previous reports [10, 11]. The unit cell dimensions of the samples obtained from XRD analysis data were listed in Table 1. It could be noticed that the a-axis value of *a* parameter decreased while the c-axis parameter *c* increased when the sintering temperature increased. This was possibly due to the presence of Na-rich phase which caused the CoO_2 layers to become less negatively charged [12].

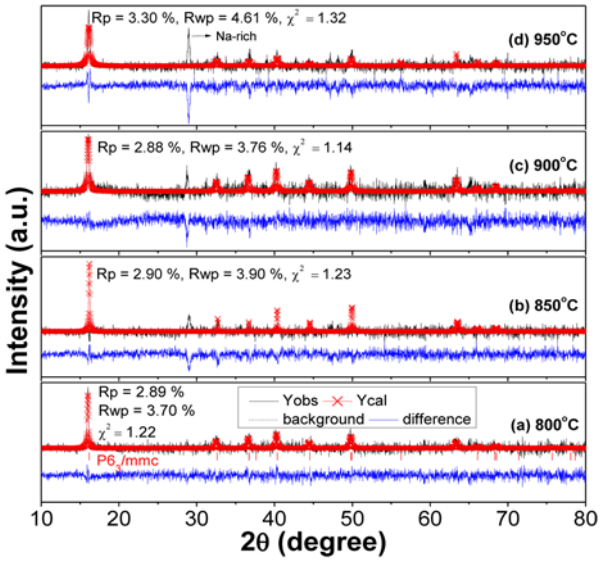

Figure 2. The simulated XRD pattern of NCO ceramics at various sintering temperatures.

Table 1. The cell parameters of $Na_{0.6}CoO_2$ ceramics.

Sintering condition	Space group	*a* (Å)	*c* (Å)	Volume of unit cell (Å^3)
800 °C /18h	$P6_3/mmc$ (No. 194)	2.8371	10.8716	75.78
850 °C /18h		2.8269	10.9539	75.81
900 °C /18h		2.8241	10.9587	75.69
950 °C /18h		2.8236	10.9818	75.82

The unit cell volume did not significantly change with increasing the sintering temperature. The chemical compositions by EDS analysis are listed in Table 2. The ceramics presented the chemical composition change with Na and O content tended to decreased, while the Co content increased with respect to Na concentration as the sintering temperature increased.

Table 2. The chemical composition values from EDS analysis of $Na_{0.6}CoO_2$.

Sintering condition	Na	Co	O
	(Atomic (%))		
800 °C /18h	22.51	18.67	58.82
850 °C /18h	23.50	23.66	52.84
900 °C /18h	18.99	25.65	55.36
950 °C /18h	11.07	38.63	50.30

To further confirm the phase structure of NCO ceramics, Raman spectroscopy was employed. The probe for analysis of local ionic configuration usually used a short length scale less than 10 nm to complement the XRD result of bulk materials [13, 14]. The results of Raman spectra of NCO are indicated in Figure 3. There were four distinct peaks observed. The Raman shift of 450, 525, 725 and 1060 cm^{-1} indicated that of O, Na, O and Na respectively, which were consistent with previous work [12]. The same number of peaks was found in the samples sintered at temperatures of 800-900 °C. However, at the sintering temperature of 950 °C, the peak position at 1060 cm^{-1} was not found which may be due to the loss of Na as this temperature was near the melting point of NCO.

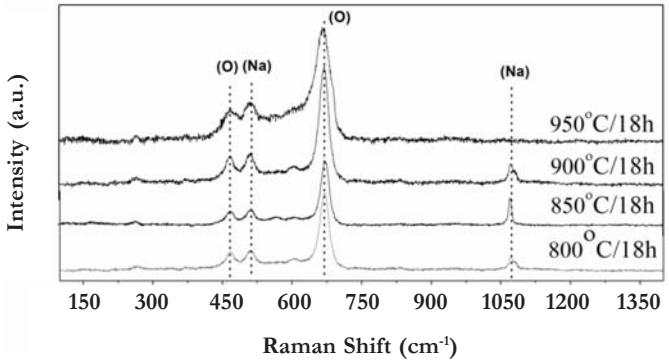

Figure 3. The Raman spectra of NCO ceramics at various sintering temperatures.

The surface microstructures of NCO ceramics are shown in Figure 4. The grains of the NCO ceramics sintered at 800 °C and 850 °C for 18 h had irregular shape. A large amount of pores were observed for these samples in agreement with their observed low densities. At the sintering temperature of 900 °C, the grains of the ceramics showed better inter-connection due to higher densification rate. The NCO ceramic sintered at 950 °C showed abnormally large grains with the presence of large pores.

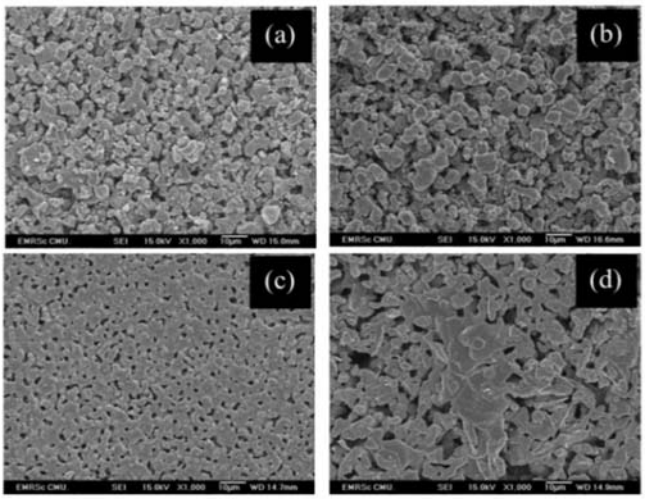

Figure 4. The SEM images of NCO ceramics sintered at (a) 800, (b) 850, (c) 900 and (d) 950 °C for 18 h.

This seemed to indicate the effect of rapid grain growth and/or partial melting. The plate sizes of the ceramic increased from about 4.1 to 7.4 μm with increasing the sintering temperature. The optimum sintering condition for NCO ceramic in normal air atmosphere investigated in this study was therefore 900 °C and 18 h and the sample was suitable for further characterization of its electrical and thermal properties.

4. CONCLUSION

Na_yCoO_2 ceramics was successfully synthesized by conventional and mixed oxide methods. The sintering condition which produced the sample with highest densities was 900 °C for 18 h under normal air atmosphere. The increase in the sintering temperature caused the opposite change in lattice parameter *a* and *c*. The Na-rich phase was also observed when sintering temperature increased. The grain size increased with increasing temperature due to the change in densification rate. The sintering temperature thus significantly affected the structural parameters and chemical stoichiometry of Na_yCoO_2 ceramics.

ACKNOWLEDGEMENTS

This work was financially supported by the Thailand Research Fund (TRF-RSA5880005) and Thailand Institute of Scientific and Technological Research. Partial supports from the Center of Excellence in Materials Science and Technology, Center of Excellence in Advanced Materials for Printed Electronics and Sensors (CMU-NECTEC), the National Research University Project under Thailand's Office of the Higher Education, the Department of Physics and Materials Science Faculty of Science and the Graduate Schools, Chiang Mai University are also acknowledged. P. Wannasut would also like to thank the financial support from the TRF through the Royal Golden Jubilee Ph.D Program (PhD 0173/2558).

REFERENCES

[1] Prasoetsopha N., Pinitsoontornand S. and Amornkitbamrung V., *Chiang Mai J.Sci.*, 2013; **40(6)**: 1030-1034.

[2] Wannasut P., Keawprak N. and Watcharapasorn A., *Chiang Mai J.Sci.*, 2018; **45(3)**: 1-6.

[3] Buntham S., Jiansirisomboon S. and Watcharapasorn A., *J. Nanosci. Nanotecnol.*, 2015; **15**: 9261-9264. DOI 10.1166/jnn.2015.11417.

[4] Seetawan T. and Seetawan A., *SNRU J. Sci. Technol.*, 2009; **1(2)**: 112-118.

[5] Terasaki I., *Phys. Rev. B.*, 1997; **56(20)**: 687-685.

[6] Stearns L.C., Zhao J. and Harmer M.P., *J. Eur. Ceram. Soc.*, 1992; **10(6)**: 473-477. DOI 10.1016/0955-2219(92)90022-6.

[7] Kraus W. and Nolze G., *J. Appl. Cryst.*, 1996; **29**: 301-303. DOI 10.1107/S0021889895014920.

[8] Lin Foo M., Wang Y., Watauchi S., Zandbergen H.W., He T., Cava R.J. and Ong N.P., *Phys. Rev. Lett.*, 2004; **92**: 247001. DOI 10.1103/PhysRevLett.92.247001.

[9] Toby B.H., *Brian Toby*, 2006; **21**: 67-70. DOI 10.1154/1.2179804.

[10] Lei Y., Li X., Liu L. and Ceder G., *Chem. Mater.*, 2014; **26**: 5288-5296. DOI 10.1021/cm5021788.

[11] Lei Y., *Determination of the Synthesis Diagram of Sodium Cobalt Oxide and Electrochemical Study*, BS Thesis, Tsinghua University, China, 2012.

[12] Takada K., Fukuda K., Osada M., Nakai I., Izumi F., Ruben A.D., Kato K., Takata M., Sakurai H., Takayama-Muromachid E. and Sasaki T., *J. Mater. Chem*., 2004; **14**: 1448-1453. DOI 10.1039/B400181H.

[13] Hao J.G., Shen B., Zhai J., Liu C., Li X. and Gao X., *J. Appl. Phys*., 2013; **113**. DOI 114106.10.1063/1.4795511.

[14] Hao J.G., Shen B., Zhai J., Liu C., Li X. and Gao X., *J. Am. Ceram. Soc*., 2013; **96**: 3133.